Geomechanics for Energy and the Environment 25 (2021) 100199

Contents lists available at ScienceDirect

Geomechanics for Energy and the Environment

journal homepage: www.elsevier.com/locate/gete

The role of ground conditions on the heat exchange potential of energy walls

Alice Di Donna [a], Fleur Loveridge [b,*], Miriam Piemontese [c], Marco Barla [c]

[a] Univ. Grenoble Alpes, CNRS, Grenoble INP, 3SR, 38000 Grenoble, France
[b] School of Civil Engineering, University of Leeds, Leeds, LS2 9JT, UK
[c] Politecnico di Torino, Dipartimento di Ingegneria Strutturale, Edile e Geotecnica, 10129 Torino, Italy

ARTICLE INFO

Article history:
Received 26 March 2020
Received in revised form 3 May 2020
Accepted 1 June 2020
Available online 3 June 2020

Editors-in-Chief:
Professor Lyesse Laloui and Professor Tomasz Hueckel

Keywords:
Energy geotechnics
Shallow geothermal energy
Numerical methods
Sustainable development
Diaphragm walls
Energy walls

ABSTRACT

Geotechnical structures are being increasingly employed, in Europe as all around the world, to exchange heat with the ground and supply thermal energy for heating and cooling of buildings and de-icing of infrastructure. Most current practical applications are related to energy piles, but embedded retaining walls are now also being adopted. However, analysis and design methods for these new dual use foundations and ground heat exchangers are currently lacking, making it hard to provide estimates of energy availability without recourse to full numerical simulation. This paper helps to fill this gap by using coupled thermo-hydro finite element analysis to develop charts of energy capacity that could be applied at the outline design stage for energy walls. In particular, the influence of ground properties (hydraulic and thermal conductivities), and ground conditions, (groundwater temperature and flow velocity) are investigated with the results showing that the hydrogeological conditions and the temperature difference between the ground source and application temperature are especially important in determining the performance of the energy wall.

1. Introduction

Underground geotechnical structures, such as deep and shallow foundations, piled and diaphragm walls, tunnel linings and anchors are being increasingly employed, in Europe as all around the world, to exchange heat with the ground and supply thermal energy for heating and cooling of buildings and de-icing of infrastructure.[1,2] The thermal activation is achieved by installing absorber pipes in the foundation, in which a circulating fluid extracts or injects heat from or into the ground. These systems belong to the category of low enthalpy geothermal plants and are combined with heat pumps and/or district heating systems. A number of practical applications of this technology are already operational especially in Austria, Germany, United Kingdom and Switzerland.[3–8]

The development of these dual use sub-structures, so called energy geostructures, started with piled foundations, and experience of energy piles now goes back over three decades.[5] Analysis and design methods have been developed both for thermal aspects[9–11] and the geomechanical considerations that follow from the additional temperature changes that will be developed within the pile.[12–14] However, recent trends in energy geostructures include the adoption of embedded retaining walls and tunnels for geothermal utilisation.[15–19] Of these types of structure, energy walls are closest to routine implementation, with the tunnel applications so far only acting as small scale trials.

However, implementation of energy walls in practice has mainly been accompanied by the use of numerical methods for thermal analysis, often in a research context.[20–24] Routine analysis and design methods for energy capacity are currently lacking. Consequently, this paper aims to provide the first design charts for energy walls based on the anticipated ground properties (hydraulic and thermal conductivities), and ground conditions (groundwater temperature and flow velocity). Section 2 provides a review of existing analysis methods and Section 3 presents the numerical model used in the paper. Sections 4 and 5 introduce the results of the analysis and present the design charts themselves, while Section 6 compares the results obtained to available field data and the performance of other energy geostructure types.

2. Analysis methods for energy walls

The first proposal for analytical methods for the design of energy walls was made by Ref. 25. Their model assumed 2D plane heat conduction within the wall and the surrounding ground. Two horizontal cross sections were used, one above and one below the excavation line, with a convective boundary condition for the inside face of the retaining wall. Point heat sources are assumed at the pipes and Green's functions used to provide a solution to the diffusion equation. The model was validated using field data

* Corresponding author.
E-mail address: f.a.loveridge@leeds.ac.uk (F. Loveridge).

https://doi.org/10.1016/j.gete.2020.100199

from the Shanghai Museum of Nature History.[26] However, at time periods under 12 h when step changes in demand are likely to occur in practice, the model fit to the field data is poor.

Ref. 27 developed and validated an analytical model for design of energy walls based on resistances and capacitors in a network set up to represent the positions of the pipes within the wall. However, numerical simulation was still required to derive the resistance values. A network approach was also used by Ref. 28 who applied the Dynamic Thermal Network (DTN) approach to energy walls. The DTN method uses a response factor approach to describe the relationship between temperature and heat fluxes at surfaces within the thermal network. However, the method requires weighting factors for heat fluxes to be calculated numerically hence limiting its routine application. Nonetheless the approach was successfully tested against a full scale field experiment.

Ref. 29 have also developed a thermal resistance model for application with energy walls. The model provides shape factors for a rectangle (the wall) with an offset hole (a heat transfer pipe). The approach is analytical, assuming either isothermal or convective boundary conditions, and could be applied with step response methods for the ground around the wall. Initial development of a step response model for walls has been undertaken by Ref. 30. However, this preliminary study is still lacking full development and validation before it can be applied.

Despite these developments, none of these methods have yet been adopted in practice. With the exception of the resistance model,[29] most require application of complex integrals, or use of numerical simulation for some sort of calibration. Furthermore, other than these few cases, reported analysis for energy walls is based entirely on numerical methods and largely based around research projects. Typically, numerical methods are based in three dimensions and used 1-dimensional special pipe elements for the heat transfer pipes and the fluid within them.[20,22,31,32] A similar approach is adopted in this paper for development of the design charts, and is described in detail in the next section.

3. Numerical model

The numerical approach used in this paper is based on the thermo-hydro mathematical formulation implemented in the finite element software FEFLOW©, with the 1D elements to represent the pipework also available in the same software.[33,34] This approach was validated for the case of energy walls by Ref. 22, by comparing against the experimental results provided by Ref. 26. A full description of the model, including governing equations is given in Ref. 22. The following sections focus instead on the details of this specific case.

3.1. Model geometry and pipes configuration

The geometry of the model is based on the literature, using average standard dimensions and considerations highlighted by Ref. 22. From literature, typical wall depths vary in the range of 10 to 40 m, while thickness is usually 0.8 to 1.2 m.[22] Thus, the approximate mean values have been selected as representative here, i.e. 20 m depth and 1 m thickness.

This type of retaining geostructure is characterised by a portion of the whole length exposed to the air of the excavation environment. It has been highlighted that the ratio between the panel height and the excavation depth does not play a major role in the energy performance of the system.[22] Consequently, for simplicity, a fixed excavation depth of 10 m was used in this analysis. The typical range of the wall panel lengths is between 2.25 and 4 m, hence a 2.5 m length panel is assumed. Fig. 1 shows a perspective view of the finite element mesh, as well as the vertical and the horizontal section of the wall. The model is 60 m high, 120 m long. This length is to allow for the inclusion of groundwater effects. In the third dimension the wall is 2.5 m wide (one panel). The model includes 405460 triangular prismatic six-node elements, 224191 nodes and a spacing between the slices in the third dimension of 0.25 m. The appropriateness of the mesh was checked through a sensitivity analysis.

The shape of the pipework installed in energy walls are quite standard and from the literature a U-shape (single or in a W-shape) can be defined to be the most common.[22,26,31,35] However, in some cases a "slinky" shape of the tube system has been chosen after optimisation analyses.[15,22,23,31] The limits for this type of pipe arrangement are construction practicalities: slinky pipework is practicable only if there are no cage joints, otherwise fusion welding is required to join the pipes every cage splice. Therefore, as a result of a compromise between construction feasibility and optimisation of heat exchange, the W-shape configuration has been selected for this analysis with a total length of the pipe of about 80 m.

Even though some previous studies indicated that installing heat exchangers also on the excavation side can be useful,[22,26] in this numerical simulation the geothermal loop will be considered on the retained side of the wall only, as is more common. The pipes are of 25 mm external diameter and 2.3 mm thickness. To have the heat absorbers installed as close as can be practically achieved to the soil, the concrete cover to the pipes is 50 mm.

Pipe spacing has proved to play a main role in the energy performance.[22] It is suggested, for the long term and a balanced heating/cooling, an optimal pipe spacing is 40–60 cm.[36] This is similar to recent analysis,[32] which recommended 50 cm to 70 cm. Therefore a representative value of 50 cm has been chosen for this model. The defined pipework configuration is represented in Fig. 1b and c.

3.2. Heat carrier fluid assumptions

The pipework was reproduced by 1D elements with a Hagen–Poiseuille law. To simulate the heat exchange process through the pipe loop, the fluid flow rate and inlet temperature must be specified. In this study, a constant inlet temperature and constant fluid flow were specified to facilitate calculation of reference heat transfer rates after a 30 day period of constant operation. This approach was taken to allow comparison of different ground conditions.

Ref. 37 show that the dependence of the heat transfer rate on the fluid velocity is not linear and for every pipe configuration an optimal velocity exists. From the experimental test conducted by Ref. 26, an optimal velocity of 0.6 to 0.9 m/s has been evaluated. However, Ref. 22 shows that, within typical values of 0.2 to 1.2 m/s, this parameter does not have a significant effect on energy performance. In this study, a value of 0.4 m/s has been used, as per.[34] Note that the model neglects the pipe resistance in the analysis. However, this value is typically small and this approach has been shown to be appropriate in previous analyses.[22]

Regarding fluid temperature, in operational conditions it will vary according to energy demand and the external temperature. For the sake of simplicity and in accordance with[34] the imposed inlet temperature in operating conditions is set equal to 4 °C for winter (heating mode) and 28 °C for summer (cooling mode) for the duration of the 30 day numerical simulations.

3.3. Material properties

Some sets of parameters were maintained as fixed within the model and some were varied as part of a sensitivity analysis. Since the aim of the analysis was to consider the effect of the

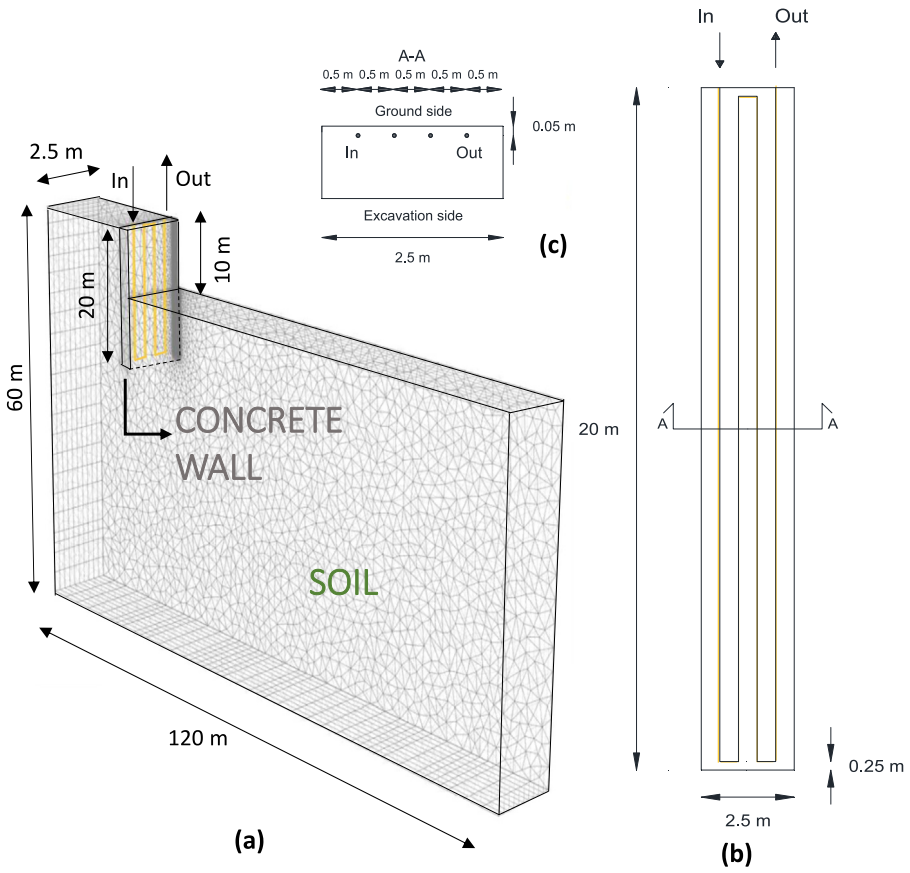

Fig. 1. Model geometry and pipes configuration: (a) 3D mesh, (b) vertical section and (c) horizontal section.

Table 1
Fixed Material properties.

Property	Concrete	Soil
Horizontal hydraulic conductivity, $k_x = k_z$ [m/s]	10^{-16}	$4.15 \cdot 10^{-3}$
Vertical hydraulic conductivity, k_y [m/s]	10^{-16}	$2.1 \cdot 10^{-4}$
Specific storage coefficient, S [m^{-1}]	10^{-4}	10^{-4}
Porosity, n [-]	0.0	0.25
Effective heat capacity ρc [$MJ/m^3/K$]	2.19	2.55
Effective thermal conductivity λ [W/m/K]	2.3	Table 2
Longitudinal dispersivity, α_L [m]	–	3.1
Transverse dispersivity, α_T [m]	–	0.3

ground conditions on the energy available, parameters pertaining to the wall concrete, fluid flow (see Section 3.2) and geometry (see Section 3.1) were fixed. Table 1 outlines all the fixed material properties, while Table 2 outlines the variable parameters. Generally the ground conditions were taken to be reflective of the in situ conditions in Torino, Italy, to be comparable to previous studies on energy tunnels[34,38]. While it is acknowledged that the concrete thermal properties may affect the outcome with some significance, this area was included in the topic of previous work and hence typical mean values were used in this analysis.

3.4. Initial hydraulic and thermal conditions

Groundwater flows are known to play a primary role in the heat transfer, because it allows a continuous thermal recharge of the ground with benefit to heat extraction and injection efficiency. It is introduced in the model by applying a hydraulic head gradient between two opposite borders of the domain, and initialising the model to get the hydraulic equilibrium (Darcy's law).

The direction of groundwater flow is another variable which should be considered.[39] Nonetheless, to limit the longitudinal dimension of the wall to a single panel, a water flow perpendicular to the wall was considered here. It is thought that in such a short extension (one wall panel only), the influence of the flowing groundwater parallel to the wall may not be correctly reproduced. It may be of interest to examine in further investigations how parallel water flow can influence the efficiency of energy walls.

The values of initial ground water flow and temperature are part of the sensitivity analysis and are given in Table 2. Different values of groundwater flow velocity are obtained by keeping permeability constant and changing the hydraulic gradient.

3.5. Boundary hydraulic and thermal conditions

A schematic representation of the adopted boundary conditions is presented in Fig. 2. The hydraulic heads imposed on the model boundaries to initialise the model are kept constant during the simulations.

The temperature on the bottom and lateral boundaries of the model is fixed equal to the initial domain temperature throughout the simulation. These boundaries were checked to be far enough away not to influence the results.

The temperature on the ground surface varies between day and night, day by day, season by season, but for simplicity, in this paper a constant value of 2 °C for winter and a constant value of 30 °C for summer were adopted. The two vertical sides, front and back of Fig. 2, are considered as adiabatic assuming interaction with adjacent wall panels.

The boundary condition on the excavation side (wall and bottom of the excavation) is expected to influence the heat exchange[22,24]. For this reason, two conditions were investigated

Table 2
Variable Material properties.

Property	Soil lower bound	Soil reference case	Soil upper bound
Effective thermal conductivity, λ [W/m/K]	0.9	2.26	3.9
Undisturbed ground temperature, T_0 [°C]	8	14	18
Groundwater flow velocity, v [m/day]	0	0	2

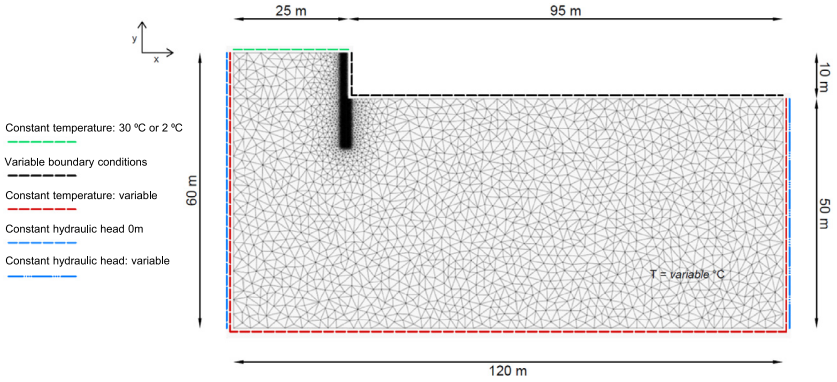

Fig. 2. Boundary conditions adopted.

in this study. Each may be taken as close to end members for the possible range of thermal behaviour:

- Fixed constant temperature (Dirichlet boundary condition) equal to 20 and 10 °C, for summer and winter respectively. This condition allows maximum heat flow across the boundary and is representative of high airflow velocity (>3–5 m/s) inside the excavation (e.g. the case of metro cut and cover tunnels and stations);[22,24]
- Imposed convective heat transfer through the wall and slab boundary (Cauchy boundary condition) q_w, such as:

$$q_w = H\,(T_{exc} - T_{wall}) \tag{1}$$

where H is the heat transfer coefficient which is reasonably varying between 2 and 20 W/m^2/K,[24] while T_{exc} and T_{wall} are the temperatures on the excavation boundary (imposed) and of the wall/slab (determined during the computation). This type of conditions allows to consider intermediate situations between an "open" boundary (i.e. imposed temperature, or H tending to infinity) and adiabatic conditions (H=0), depending on the value of the heat transfer coefficient. Imposing constant temperature could be non-conservative with respect to heating capacity, although if airflow in the excavation is faster than 3 to 5 m/s (as it might occur for instance in cut and cover tunnels), this assumption will not be too far in error. Studies where a heat transfer coefficient approach is adopted are summarised in Ref. 22, together with the evaluation of appropriate H values. Justification for this approach can also be found in ISO 6946[40] where surface heat transfer coefficients are provided for internal and external spaces in the built environment. ISO 6946 also gives guidance on linking air speeds to heat transfer coefficients. Data related to tunnel internal temperature are also available in the literature and are summarised in Refs. 22, 41. These vary seasonally, generally in response to the external air temperature, and are usually higher than the original undisturbed ground temperature. Based on these considerations, in this study, the coefficient H was assumed equal to 2.5 W/m^2/K, to represent a lower bound heat transfer condition, while not being as conservative as an adiabatic condition[42] that may be unlikely to occur in reality. T_{exc} was fixed to 20 and 10 °C, for summer and winter respectively. This condition is representative of near-zero airflow velocity inside the excavation (basement and underground parking).

3.6. Simulation steps

After the hydraulic initialisation, the operational conditions of the geothermal system were simulated by circulating the fluid in the pipes at a given inlet temperature and velocity. Each simulation lasted 30 days. The heat Q (expressed in W) extractable during winter and injectable during summer was computed as:

$$Q = mc_w\,|T_{wo} - T_{wi}| \tag{2}$$

where m is the mass flow rate expressed in kg/s, c_w is the circulating fluid heat capacity in J/kg/K, T_{wi} is the inlet (imposed) temperature of the pipe circuit and T_{wo} the outlet temperature (result of the numerical simulation). In this paper, the circulating fluid is assumed to be water and c_w is taken equal to 4200 J/kg/K.

4. Results

The effect of the three investigated parameters are discussed and quantified in the following paragraphs, for both the thermal boundary conditions on the excavation side.

4.1. Reference case

As a reference condition, the case with initial soil temperature equal to 14 °C, no underground water flow and bulk soil thermal conductivity of 2.26 $W/m/K$ was considered. The results in terms of heat exchanged (Eq. (2)) during one month simulation are presented in Fig. 3, for winter and summer conditions, and for both the thermal boundary conditions assumed on the excavation side. The heat exchange per unit surface area of the wall in contact with the ground is considered, i.e. Q is divided by 20 × 2.5 m^2, for the sake of comparing with other theoretical studies, field data, and generalising the results. The heat exchange of the upper part of the wall (exposed to air on one side), and the embedded lower part are therefore considered together. This approach is supported by the results presented in Ref. 22, where the effect of the ratio between the panel height and the excavation depth on the heat exchange potential was investigated. Varying this ratio between 1.25 and 2, the authors concluded that it has limited

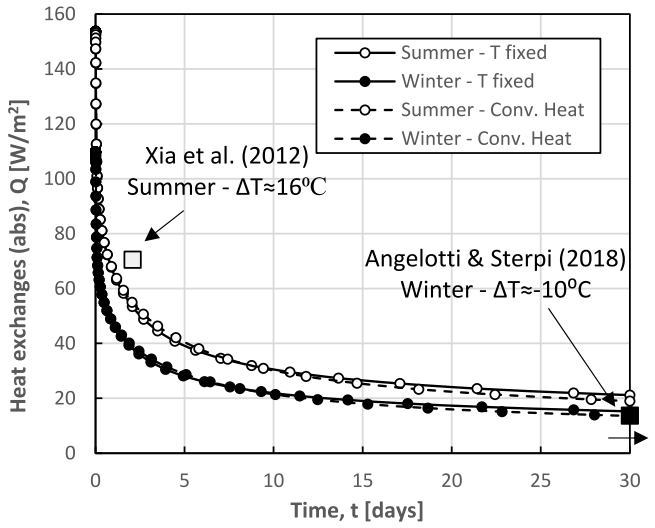

Fig. 3. Heat injected/extracted during 30 days simulation for the reference case ($T_s = 14°C$, $T_{wi} = 28°C$ or $4°C$) compared with literature data.

importance on the heat exchange potential of the wall panel in the long term, compared with other design parameters.

For the fixed temperature boundary condition, at the end of the 30 days, the difference in temperature between the inlet and the outlet of the pipes circuit was 1.9 °C and 1.4 °C for summer and winter respectively, resulting in values of exchanged heat of 21.2 W/m^2 (injected) and 15.3 W/m^2 (extracted). For the heat convective boundary conditions, the difference in temperature between the inlet and the outlet of the pipes circuit was 1.7 °C and 1.2 °C for summer and winter respectively, resulting in values of exchanged heat of 19.1 W/m^2 (injected) and 13.6 W/m^2 (extracted). These values (Table 3) confirm a reduced efficiency in the case of convective heat boundary condition by approximately 10 to 12%, due to the limited heat exchange allowed on the excavation side, with respect to the temperature fixed boundary condition. However, the bigger difference in performance is between the summer and winter conditions. The better performance of the system in summer was expected due to the higher absolute difference between the inlet and the initial ground temperature ($|\Delta T|$), which was of 14 °C in summer and 10 °C in winter.

Monitoring data of existing operating systems are generally limited in the literature[2,43]. Among the data available, the only comparable with the numerical results were found to be those presented by Ref. 16 and Ref. 26. To consider comparable conditions between the monitoring data and the numerical computations, it is worth considering the difference in temperature between the undisturbed soil and the inlet:

$$|\Delta T| = T_{wi} - T_s \tag{3}$$

In the simulations realised in this work, it was equal to 14 and 10 °C, for summer and winter respectively. Ref. 16 reported monthly heat extraction values between 12.5 and 14.9 W/m^2 for a real scale and operational diaphragm wall heat exchanger in a building basement, with soil bulk thermal conductivity of 2.2 W/m/K, inlet temperature around 4 °C and monitored soil temperature of 13.4 °C ($|\Delta T| \approx 10$ °C), which is reasonably comparable with the 13.6 W/m^2 and 15.3 W/m^2 found in this work for the convective heat boundary condition and for the fixed temperature boundary condition respectively.

Ref. 26 carried out field thermal performance tests of a W shaped diaphragm wall heat exchanger with heat injection values between 68 W/m^2 and 73 W/m^2, for a bulk thermal conductivity of 2.34 W/mK, an inlet temperature of 32 °C and undisturbed soil temperature of 16.3 °C ($|\Delta T| \approx 16$ °C). Fig. 3 highlights that the difference between the two cases is not that significant. Some of this difference is due to a higher $|\Delta T|$ in the field experiment, but the larger effect is likely to be the test duration (Ref. 26 ran their test for only 50 h, compared to the one month long simulation).

It is interesting to compare these results with those obtained on energy tunnels through the same approach and under the same conditions (T_s=14 °C, $\lambda = 2.26$ W/m/K, no ground water flow, T_{wi}=4/28 °C for winter/summer, fluid velocity of 0.4 m/s, fixed temperature boundary condition). The results in terms of heat exchange are surprisingly similar (refer also to Section 6). In the case of an energy tunnel, the heat extracted/injected was 11.4/16.0 W/m^2[34], so slightly lower than 15.3/21.2 W/m^2 obtained in this case for the fixed temperature boundary. Since this difference is small, it could relate to geometric factors such as the pipe arrangements and spacing (which is 30 cm rather than 50 cm), tunnel curvature, and absence of the embedded section with soil on both sides of the structure. All these factors are known to effect the heat availability in energy geostructures (e.g. Refs. 22, 43).

4.2. Influence of ground temperature

The simulation was repeated by varying the undisturbed ground temperature between 8 and 18 °C and keeping all the other parameters unchanged. The heat exchanged values at the end of a one-month period simulation, for summer and winter conditions, and for the two mentioned excavation-side boundary conditions are compared in Fig. 4a, as a function of the undisturbed ground temperature. In summer, the increase in soil temperature reduces the temperature difference between the undisturbed ground and the inlet (which is constant at 28 °C), and as a result the efficiency decreases. The opposite trend is shown in winter mode. As already observed, the heat transfer boundary condition limits the heat exchange through the excavation boundary, induces a temperature increase/decrease in summer/winter on the wall internal boundary, and a consequent decrease of total heat exchange. The measurements presented by Ref. 16 are in good agreement. The variation of the injected/extracted heat with undisturbed ground temperature is linear, as highlighted in Fig. 4b which shows the relationship between the heat exchanged and the absolute temperature difference between the fluid entering the wall and the ground undisturbed temperature. This also demonstrates that the direction of heat transfer (i.e. the season) is unimportant and that this absolute difference ($|\Delta T|$) is the key factor.

4.3. Influence of thermal conductivity

The second parameter that was investigated was the bulk thermal conductivity of the soil, varying between 0.9 $W/m/K$ and 3.9 $W/m/K$. The heat exchanged at the end of a one-month simulation, for summer and winter conditions, and for the two internal air boundary conditions are compared in Fig. 5 as a function of thermal conductivity. In all conditions, the expected increase of exchanged heat with the thermal conductivity is more significant in summer (where $|\Delta T|$ is higher) for both boundary conditions. The influence of the excavation boundary condition is limited in this case: the increase in heat exchange is roughly independent on the boundary condition assumed. The measurements presented by Ref. 16 are once again in good agreement and seem to be better reproduced by the heat convective boundary condition.

Table 3
Heat exchange results after 30 days simulation (reference case).

	Excavation BC	T_s	T_{wi} [°C]	$\|\Delta T\|$	T_{wo} [°C]	Q [W/m^2]
Summer	T fixed Conv. Heat	14	28	14	26.07 26.27	21.20 19.03
Winter	T fixed Conv. Heat	14	4	10	5.39 5.24	15.27 13.58

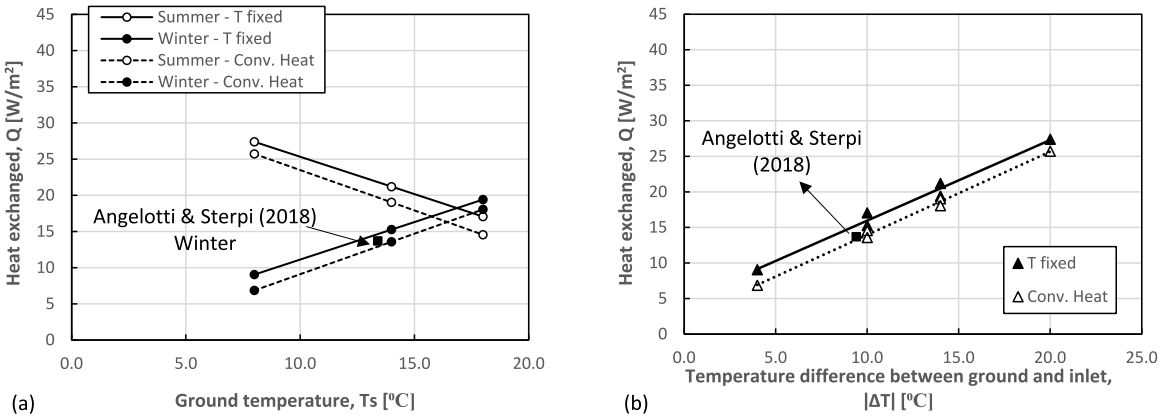

Fig. 4. (a) Effect of ground initial temperature on the heat exchange with constant temperature boundary conditions (continuous lines) and convective boundary conditions (dashed lines) in W/m^2. (b) Effect of absolute temperature difference on heat exchanged for both boundary conditions.

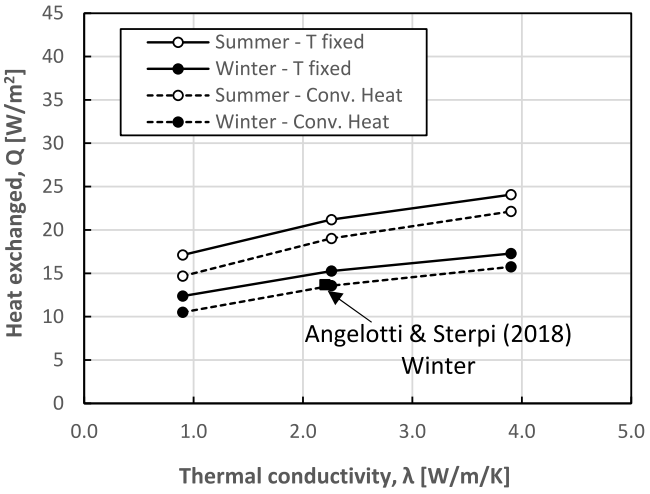

Fig. 5. Effect of ground thermal conductivity on the heat exchange with constant temperature boundary conditions (continuous lines) and convective boundary conditions (dashed lines) in W/m^2.

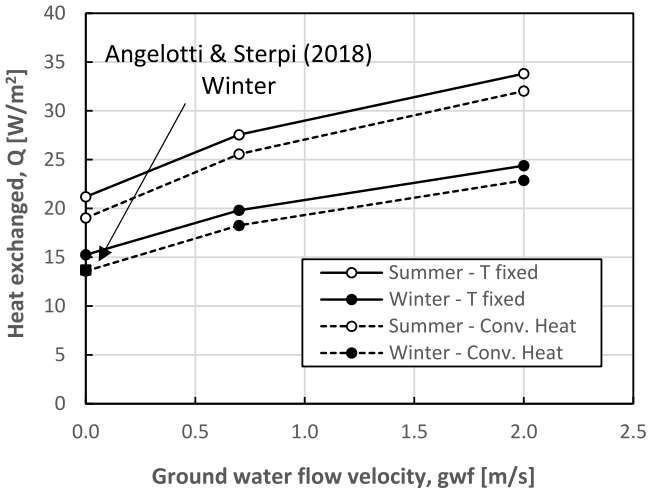

Fig. 6. Effect of ground water flow velocity on the heat exchange with constant temperature boundary conditions (continuous lines) and convective boundary conditions (dashed lines) in W/m^2.

4.4. Influence of ground water flow velocity

Fig. 6 illustrates the effect of groundwater flow velocity ranging between 0 m/day (reference case) and 2 m/day on the energy efficiency of the system, for winter and summer modes and both the excavation side boundary conditions. As expected, both in heating and cooling mode, the exchanged heat increases in a non-linear way with the increasing of groundwater flow velocity. This increase is much less significant than for the case of energy tunnels, where[34] show the heat transfer rates in the presence of groundwater flow to reach maximum values of 57.7 W/m^2 and 80.7 W/m^2 in the winter and in the summer respectively, under identical soil thermal conductivity, permeability, hydraulic gradient and temperature. This difference is thought to be due to the geometry of these structures (Fig. 7): the wall actually acts as a dam, limiting considerably the flow along the wall face and the consequent beneficial thermal recharge. Fig. 7 shows that the far field flow rate of 1.4 m/day is reduced to only 1 cm/day near the top of the wall because of the dam effect. The corresponding flow vectors concentrate around the toe of the wall, from which relatively little heat transfer occurs compared with the wall faces. By comparison, for the tunnel case, the flow vectors concentrate at the invert and crown and therefore provide more advantageous heat transfer conditions. If the groundwater flow would run parallel to the length of the energy wall, then the dam effect would be reduced and the evaluation of the energy availability would differ, potentially offering higher heat transfer rates. Nonetheless the scenario analysed remains a suitable conservative case for first assessment.

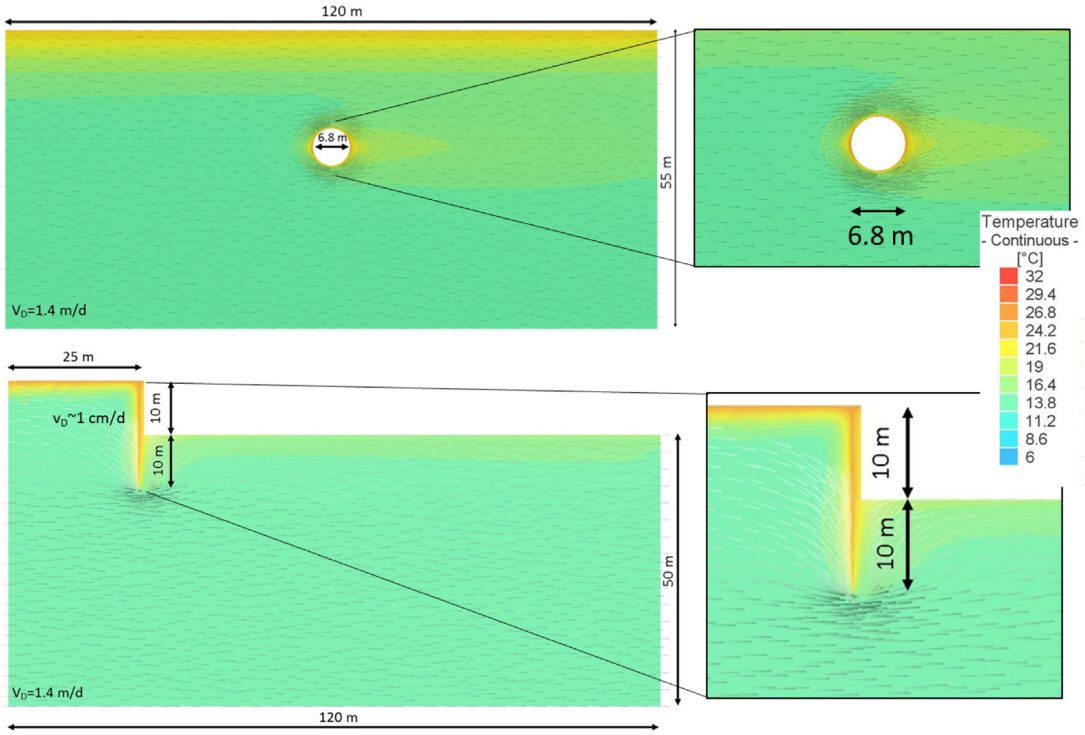

Fig. 7. Temperatures and groundwater streamlines vectors illustrating the dam effect for an energy tunnel and an energy wall in presence of underground far field water flow of 1.4 m/day.

5. Preliminary design charts

Bringing together all these results with a full factorial analysis of the cases[44], design charts were developed. They are presented in Figs. 8 and 9 for constant temperature and convective heat boundary condition on the excavation side, respectively. On the basis of the specific site conditions, i.e. ground temperature, soil thermal conductivity and groundwater flow velocity, the charts give an indication of the heat that can be potentially extracted/injected, expressed in watts per square meter of wall surface. They are obviously related to the specific geometry and assumptions of the presented model, but could be used as a preliminary assessment.

5.1. Effect of the excavation boundary condition

To better evaluate the importance of the selected boundary conditions on the excavation side, other design charts were plotted for the case of thermal conductivity equal to 2.26 $W/m/K$ including in the same graph the results for the two boundary conditions (Fig. 10). For the same initial soil temperature and underground water flow velocity, the constant temperature boundary condition always gives a higher heat exchange, but the increment with respect to the heat transfer boundary condition is not always the same. The percentage difference between the two conditions is defined as:

$$D = \frac{Q_T - Q_H}{Q_H} \cdot 100 \tag{4}$$

where Q_T and Q_H are the heat exchanged with constant temperature and heat transfer boundary conditions respectively. The difference is greatest for no groundwater flow and for lower absolute difference between the inlet temperature and the ground temperature. The smallest percentage difference is 2.5% with a temperature difference between the soil and the ground of 20 °C and underground water flow velocity of 2 m/d, while the highest is 31.9% with a temperature difference between the soil and the ground of 4 °C and no underground water flow.

6. Discussion and comparison with other energy geostructures

The preliminary design charts demonstrate that the two most important factors in assessing initial capacity are the absolute temperature difference between the circulating fluid and the ground, and the presence or absence of significant groundwater flow. For example the former can increase the heat exchange from 9 W/m^2 to 27 W/m^2 as the temperature differences increases from 4 °C to 20 °C (see Fig. 4b) for the fixed temperature boundary condition. Similar results are observed for the convective case. The latter is seen to increase energy availability by between 150% and 200% depending on the case, and could be even more important in the case of flow parallel to the length of the structure. The ground thermal conductivity is also important when groundwater flow is absent, leading to a similar 150% increase in capacity over the range of parameters studied. While the nature of the internal boundary condition does impact the results obtained, this effect is typically smaller than the influence of the ground conditions.

Overall the results of the analysis presented give an extreme range of heat transfer rates between 6 W/m^2 and 32 W/m^2 in the absence of groundwater flow, increasing to 48 W/m^2 where that flow is significant. Therefore, overall a reasonable typical range of 15 to 25 W/m^2 could be inferred from the base case.

It has already been observed that these figures are in line with field data obtained for energy walls in other studies, especially when considering the duration of those trials and the absolute temperature difference. These figures can be further compared to field data from other energy geostructures. Three energy tunnel field trials of lengths of one month or more are summarised in Ref. 43. The cases presented heat transfer rates in the range 3 W/m^2 to 34 W/m^2. This range is close to the extreme range of values determined in this study. It is a wider range than

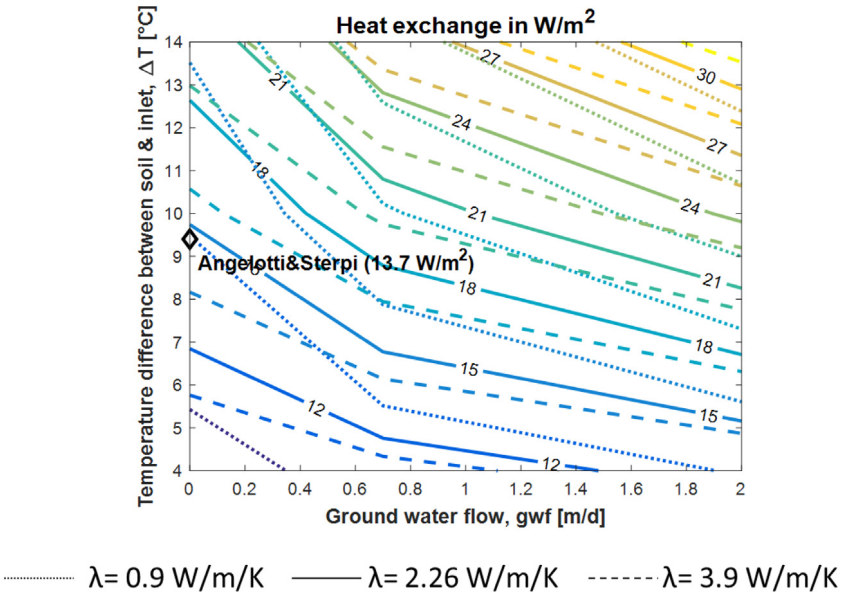

Fig. 8. Design charts for constant temperature BC (values in W/m^2).

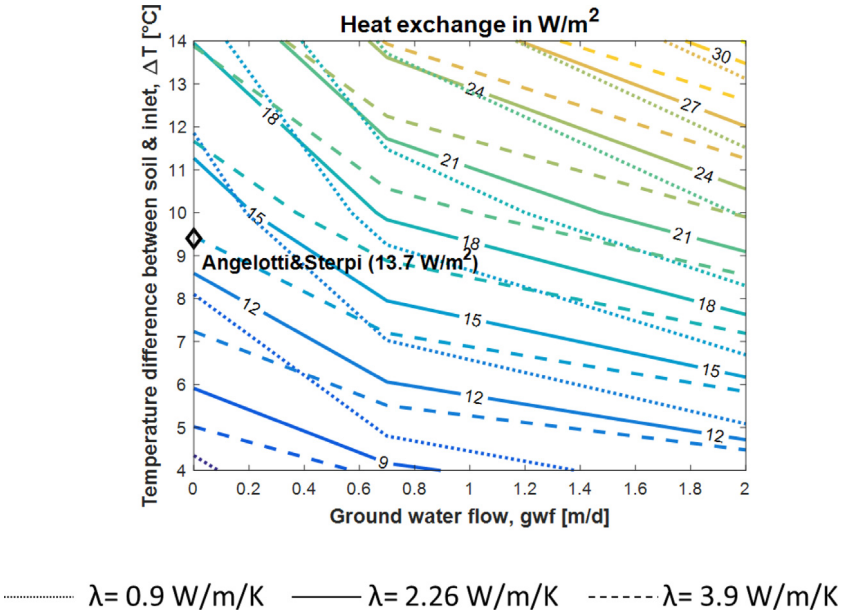

Fig. 9. Design charts for heat transfer BC (values in W/m^2).

the field data for energy walls, perhaps relating to the larger number of cases. This is therefore consistent with the results of the numerical studies, providing very similar ranges of energy availability for tunnels and walls.

Four long term studies of energy availability from energy piles are also included in Ref. 43. Here the results are in the range from 21 W/m^2 to 46 W/m^2 and is noticeably higher than the data from walls and tunnels, especially at the lower bound. This increased capacity per foundation surface area will be related to the full embedment of energy piles, and the absence of the excavations side boundary condition which can effect the efficiency of energy wall and energy tunnel schemes.

7. Conclusions

This study has presented preliminary design charts for outline design of energy walls, focusing on the role of the initial ground conditions. The most important factors determining the energy availability from an embedded retaining wall used as a heat exchanger are:

- The undisturbed ground temperature relative to the fluid circulation temperature in the wall. This absolute temperature difference can have a threefold impact on the energy exchanged under the conditions studied.
- The groundwater flow velocity, which can increase the energy available by 150% or more compared with the case of no flow. However, the cases considered with groundwater flow perpendicular to the wall length showed the wall to act partially as a dam, restricting groundwater benefit compared to other energy geostructures. This effect would be less significant for water flow parallel to the tunnel length in which case the beneficial effect of groundwater flow would be higher.

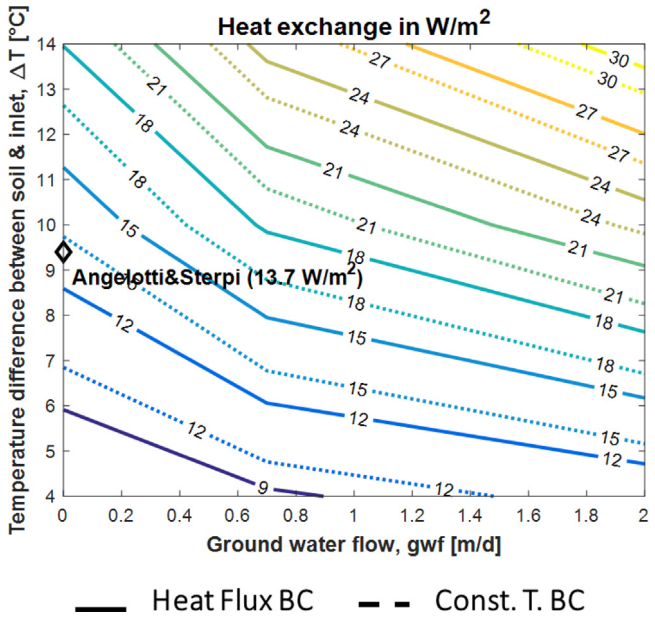

Fig. 10. Design charts: comparison between constant temperature and heat transfer boundary conditions ($\lambda = 2.26$ W/m/K).

- The ground thermal conductivity, which in the absence of groundwater flow can also increase the energy availability by up to 150%.

It is also important to consider appropriate excavation side boundary conditions, as this study showed that choices made here can lead to differences in outcome of up to 32%. This means giving proper consideration to the use of the space made by the retaining structure, whether it is temperature controlled, or perhaps subject to air flow movements or other sources of heat.

Overall, it can be shown that reasonable values for first assessment of energy wall capacity would be in the range 15–25 W/m^2. The presented design charts could then be used for a site specific first assessment, prior to carrying out a full design of the system.

CRediT authorship contribution statement

Alice Di Donna: Conceptualization, Methodology, Writing - original draft, Writing - review & editing, Visualization, Supervision, Funding acquisition. **Fleur Loveridge:** Writing - original draft, Writing - review & editing, Supervision, Funding acquisition. **Miriam Piemontese:** Validation, Formal analysis, Investigation, Visualization, Writing - original draft. **Marco Barla:** Conceptualization, Methodology, Writing - review & editing, Supervision, Funding acquisition, Project administration, Resources.

Declaration of competing interest

The authors declare that they have no known competing financial interests or personal relationships that could have appeared to influence the work reported in this paper.

Data statement

The output data associated with this paper are openly available from the University of Leeds Data Repository at https://doi.org/10.5518/830.

Acknowledgements

This work was carried out in the framework of the Cost Action GABI TU 1405, European network for shallow geothermal energy applications in buildings and infrastructures. The authors are also grateful for additional funding from the Royal Academy of Engineering in the UK, EPSRC (grant reference EP/S001417/1) and from the Politecnico di Torino, Italy (Assegnazioni di Ateneo per la ricerca di base). The laboratory 3SR is part of the LabEx Tec 21 (Investissement d'avenir — grant agreement n. ANR-11-LABX-0030).

References

1. Laloui L, Di Donna A. *Energy Geostructures: Innovation in Underground Engineering*. ISTE Ltd and John Wiley & sons Inc; 2013.
2. Di Donna A, Barla M, Amis T. Energy geostructures: Analysis from research and systems installed around the World. In: *DFI 42th Annual Conference on Deep Foundations*. New Orleans, USA; 2017.
3. Adam D. Tunnels and foundations as energy sources - Practical applications in Austria. In: *5th International Symposium on Deep Foundations on Bored and Auger Piles (BAP V)*; 2009:337–342.
4. Bourne-Webb PJ. Observed behaviour of energy geostructures. In: Laloui L, Di Donna A, eds. *Energy Geostructures: Innovation in Underground Engineering*. ISTE Ltd and John Wiley & Sons Inc.; 2013.
5. Brandl H. Energy foundations and other thermo-active ground structures. *Géotechnique*. 2006;56(2):81–122.
6. Pahud D. A case study: the dock midfield of zurich airport. In: Laloui L, Di Donna A, eds. *Energy Geostructures: Innovation in Underground Engineering*. ISTE Ltd and John Wiley & Sons Inc; 2013, 281–295.
7. Riederer P, Evers G, Gourmez D, Jaudin F, Monnot P, Pertenay V, Pincemin S, Wurtz E. *COnception de FOndations GEothermiques*. 2007, 170.
8. SIA DO 190. *Utilisation de la Chaleur Du Sol Par Des Ouvrages de Fondation Et de Soutènement En Béton. Guide Pour la Conception, la Realization Et la Maintenance*. Switzerland: Société Suisse des ingénieurs et des architects; 2005.
9. Pahud D. *PILESIM: Simulation Tool for Heating / Cooling Systems*. 2007.
10. Alberdi-Pagola M, Poulsen SE, Jensen RL, Madsen S. A case study of the sizing and optimisation of an energy pile foundation (Rosborg, Denmark). *Renew Energy*. 2018;147:2724–2735.
11. Loveridge F, Powrie W. Temperature response functions (G-functions) for single pile heat exchangers. *Energy*. 2013;57:554–564.
12. Mimouni T, Laloui L. Behaviour of a group of energy piles. *Can Geotech J*. 2015;52(12):1913–1929.
13. Rotta Loria AF, Laloui L. The interaction factor method for energy pile groups. *Comput Geotech*. 2016;80:121–137.
14. Di Donna A, Laloui L. Numerical analysis of the geotechnical behaviour of energy piles. *Int J Numer Anal Methods Geomech*. 2014;39:861–888.
15. Amis T, Robinson CAW, Wong S. Integrating geothermal loops into the diaphragm walls of the knightsbridge palace hotel project. In: *Proceeding of the 11th DFI / EFFC International Conference, London*; 2010:10.
16. Angelotti A, Sterpi D. On the performance of energy walls by monitoring assessment and numerical modelling: a case in Italy. *Environ Geotech*. 2018;1–8.
17. Adam D, Markiewicz R. Energy from earth-coupled structures, foundations, tunnels and sewers. *Géotechnique*. 2009;59(3):229–236.
18. Franzius JN, Pralle N. Turning segmental tunnels into sources of renewable energy. *Proc Inst Civ Eng*. 2011;164(1):35–40.
19. Barla M, Di Donna A, Insana A. A novel real-scale experimental prototype of energy tunnel. *Tunnell Underground Space Technol*. 2019;87:1–14.
20. Narsilio G, Makasis N, Bidarmaghz A, Disfani M. *Geo-Exchange Feasibility Study – Phase 2: Parkville Metro Station*. Melbourne (Vic), Australia: MMRA; 2016.
21. Rammal D, Mroueh H, Burlon S. Thermal behaviour of geothermal diaphragm walls: Evaluation of exchanged thermal power. *Renew Energy*. 2018;147:2643–2653.
22. Di Donna A, Cecinato F, Loveridge F, Barla M. Energy performance of diaphragm walls used as heat exchangers. *Proc Inst Civ Eng*. 2016;170(3):1–14.
23. Barla M, Di Donna A, Santi A. Energy and mechanical aspects on the thermal activation of diaphragm walls for heating and cooling. *Renew Energy*. 2018;147(2):2654–2663.
24. Bourne-Webb PJ, Bodas Freitas TM, Da Costa Gonçalves RA. Thermal and mechanical aspects of the response of embedded retaining walls used as shallow geothermal heat exchangers. *Energy Build*. 2016;125:130–141.
25. Sun M, Xia C, Zhang G. Heat transfer model and design method for geothermal heat exchange tubes in diaphragm walls. *Energy Build*. 2013;61:250–259.

26. Xia C, Sun M, Zhang G, Xiao S, Zou Y. Experimental study on geothermal heat exchangers buried in diaphragm walls. *Energy Build*. 2012;52:50–55.
27. Kurten S, D. Mottaghy, Ziegler M. A new model for the description of the heat transfer for plane thermo-active geotechnical systems based on thermal resistances. *Acta Geotech*. 2015;10(2):219–229.
28. Shafagh I, Rees S, Mardaras IU, Janó MC, Carbayo MP. A model of a diaphragm wall ground heat exchanger. *Energies*. 2020;13(2):1–23.
29. Shafagh I, Rees SJ. Analytical investigations into thermal resistance of diaphragm wall heat exchangers. In: *Proceedings of the European Geothermal Congress, EGC 2019, (11–14 June)*; 2019:1–6.
30. Shafagh I, Loveridge F. Developing analysis approaches for energy walls. In: *2nd International Conference on Energy Geotechnics*. La Jolla, California, USA; 2020.
31. Sterpi D, Coletto A, Mauri L. Investigation on the behaviour of a thermo-active diaphragm wall by thermo-mechanical analyses. *Geomech Energy Environ*. 2017;9:1–20.
32. Makasis N, Narsilio GA. Energy diaphragm wall thermal design: the effects of pipe configuration and spacing. *Renew Energy*. 2020;154:476–487.
33. Diersch HJG. *DHI Wasy Software - Feflow 6.1 - Finite Element Subsurface Flow & Transport Simulation System: Reference Manual*. 2009.
34. Di Donna A, Barla M. The role of ground conditions on energy tunnels' heat exchange. *Environ Geotech*. 2016;3(4):214–224.
35. Unterberger W, Hofinger H, Adam Roman, Markiewics Roman. Utilization of Tunnels as Sources of Ground Heat and Cooling–Practical Applications in Austria. In: *Proceedings of the ISRM international Symposium 3rd ARMS*; 2004:421–426.
36. ICConsulten. *Wirtschaftliche Optimierung VonTunnelthermie Absorberanlagen*. Vienna, Austria: Grundlagenuntersuchungund Planungsleitfaden; 2005, (in German).
37. Sterpi D, Angelotti A, Conti D, Ramus M. Numerical analysis of heat transfer in thermo-active diaphragm walls. In: Hicks MA, Brinkgreve RBJ, Rohe A, eds. *Numerical Methods in Geotechnical Engineering*. USA: CRC Press; 2014, 1043–1048.
38. Insana A, Barla M. Experimental and numerical investigations on the energy performance of a thermo-active tunnel. *Renew Energy*. 2020;152:781–792.
39. Delerablee Y, Burlon S, Reiffsteck P. Long-term assessment of thermal sustainability of thermoactive geostructures. *Environ Geotech*. 2019;1–17.
40. ISO 6946:2017. *Building Components and Building Elements – Thermal Resistance and Thermal Transmittance – Calculation Method*. International Standards Organisation; 2017, 40.
41. Nicholson DP, Chen Q, Pillai A, Chendorain M. Developments in thermal piles and thermal tunnel lining for city scale GSHP systems. In: *Thirty-Eighth Workshop on Geothermal Reservoir Engineering*; 2013.
42. Makasis N, Narsilio GA, Bidarmaghz A, Johnston IW, Zhong Y. The importance of boundary conditions on the modelling of energy retaining walls. *Comput Geotech*. 2020;(120).
43. Loveridge F, McCartney JS, Narsilio GA, Sanchez M. Energy geostructures: A review of analysis approaches, in situ testing and model scale experiments. *Geomech Energy Environ*. 2020;100173.
44. Di Donna A, Loveridge F, Piemontese M, Barla M. The role of ground conditions on the heat exchange potential of energy walls – data. University of Leeds. 2020. https://doi.org/10.5518/830.